One-step solid-state synthesis of Cu_2O/Bi_2O_3 nanocomposite at room temperature and its enhanced photocatalytic activity under visible light irradiation

L. LI, J. JIANG, X. LUAN, C. FENG, Q. YANG, M. CHEN, M. ZHANG*

School of Chemistry and Materials Science, Huaibei Normal University, Huaibei 235000, China

A novel visible-light-driven Cu_2O/Bi_2O_3 nanocomposite photocatalyst was fabricated at room temperature via a simple mild one-step solid-state reaction method. The as-synthesized products were characterized by X-ray powder diffraction and UV–Vis diffuse reflectance spectroscopy. The results showed that the as-synthesized Cu_2O/Bi_2O_3 nanocomposite was composed of cubic Cu_2O and monoclinic alpha-Bi_2O_3 with a good visible-light absorption performance. The Cu_2O/Bi_2O_3 nanocomposite can be used for the degradation of methyl orange at room temperature under visible light irradiation. The photocatalytic activity of Cu_2O/Bi_2O_3 was higher than that of the pure Cu_2O and Bi_2O_3. Based on the band gap structures of Cu_2O and Bi_2O_3, the enhanced photocatalytic activity of the composite can be attributed to the efficient separation of photogenerated electrons and holes.

(Received February 2, 2015; accepted March 19, 2015)

Keywords: Bi_2O_3, Cu_2O, Composites, Solid-state reaction, Photocatalytic activity

1. Introduction

Heterogeneous photocatalysis based on semiconductor materials is a promising technology that offers numerous applications in environmental pollution purification and energy conversion [1, 2]. Among a variety of semiconductor photocatalysts, TiO_2 is the most intensely investigated due to its non-toxicity and chemical stability. But the wide band gap of TiO_2 (3.2 eV for anatase), which is only responsive to ultraviolet (UV) irradiation, restricts its practical application. In recent years, developing visible-light-driven photocatalysts has attracted a considerable concern, since the use of visible-light-driven photocatalysts will both improve the outdoor photocatalytic activity and enable the extension of the indoor applications where there is almost no UV irradiation [3]. Bismuth oxide (Bi_2O_3) appears to be a good visible light photocatalyst candidate, because it has strong response to visible light owing to its small direct band gap (~2.8eV) [4]. Unfortunately, pure Bi_2O_3 shows poor photocatalytic activity for the decomposition of organic pollutants due to the fast recombination of the photoinduced electrons and holes [5-7]. One of the ways to improve the separation of the photoinduced charge carriers is to combine Bi_2O_3 with a semiconductor of appropriate band position [8]. With successful cases such as Bi_2O_3-$BiVO_4$ [8], Bi_2O_3-Bi_2WO_6 [9], NiO-Bi_2O_3 [10], BiOCl/Bi_2O_3 [11], BiOI/Bi_2O_3 [12], Ag_2O-Bi_2O_3 [13] and Fe_2O_3/Bi_2O_3 [14] in mind, we attempt to couple Cu_2O with Bi_2O_3 to obtain Cu_2O/Bi_2O_3 composites.

Cu_2O is a p-type semiconductor with a direct band gap of ~2.2eV [15]. The conduction band edge of Cu_2O is much higher than that of Bi_2O_3. When Cu_2O and Bi_2O_3 are compounded to form composites, the photoinduced electrons can transfer from the conduction band of Cu_2O to that of Bi_2O_3 under light irradiation, while the photoinduced holes in Bi_2O_3 can transfer to the valence band of Cu_2O, improving the separation of photogenerated electrons and holes [4]. Accordingly, the enhancement of the photocatalytic activity of both Bi_2O_3 and Cu_2O can be achieved.

Recently, Abdulkarem et al. [4] first synthesized Bi_2O_3/Cu_2O composites using hydrothermal method. Here, we present a much simpler and milder method to prepare Cu_2O/Bi_2O_3 composites. Our approach employ a rapid one-step solid-state ball milling reaction at room temperature, avoiding the long annealing times compared to the above hydrothermal method. To the best of our knowledge, the method for preparing Cu_2O/Bi_2O_3 nanocomposite in this paper has never been reported. We also evaluate the photocatalytic activities of Cu_2O/Bi_2O_3 compared with those of pure Bi_2O_3 and Cu_2O by decomposing methyl orange under visible light irradiation. The results show that the as-synthesized Cu_2O/Bi_2O_3 nanocomposite exhibits much better photocatalytic activity than its single component. We expect that the study will develop a new route to synthesize Cu_2O/Bi_2O_3 nanocomposite with the enhancement of the photocatalytic activity, and provide a clue for modification of semiconductor as well.

2. Experimental

2.1. Synthesis of the Cu_2O/Bi_2O_3 composites

All chemicals used in the study were of analytical grade quality and were used directly without further purification. In a typical synthesis process, the initial reactants CuCl, $Bi(NO_3)_3{\cdot}5H_2O$ and NaOH were firstly mixed together in agate ball milling tanks with a molar ratio of 1:3:13. Then, the mixture was allowed to have a ball milling reaction using the planetary ball mill (QM-3SP04, China) at the rotation speed of 480 rpm for a certain time at room temperature. Finally, the ball-milled product was washed with water, and dried under vacuum at 60 °C for 4 h to get Bi_2O_3/Cu_2O composites.

2.2. Characterization

A X-ray powder diffractometer (Bruker D8 Advance, Germany) with Cu Kα radiation (λ= 0.15406 nm), the accelerating voltage of 40 kV and the emission current of 40 mA was used to determine the crystal phase composition and the crystallite size of the synthesized samples. And a UV-visible spectrophotometer equipped with an integrating sphere (TU-1901, Beijing Purkinje General Instrumental Co., China) was employed to obtain the UV-Vis diffuse reflectance spectroscopy.

2.3. Photocatalytic activity test

The photocatalytic degradation experiments were carried out in a photochemical reactor using a 500 W Xenon lamp with a 420-nm UV cutoff filter as a light source. The photocatalytic performance of the prepared Cu_2O/Bi_2O_3 composite was evaluated by the photodegradation of methyl orange (MO) under visible light irradiation at room temperature which was kept by cooling water to prevent any thermal catalytic effect. In a typical photodegradation process, 0.1 g of the prepared Cu_2O/Bi_2O_3 photocatalyst was dispersed in 100 ml of MO aqueous solutions with an initial concentration of 10 mg/L. Prior to irradiation, the suspension was stirred in dark for 60 min to establish adsorption–desorption equilibrium between photocatalyst and MO, and then was exposed to light under stirring. At given time intervals, small quantities of the solution were withdrawn, centrifuged and subsequently filtered through a 0.2 μm millipore filter to separate the catalysts from the reaction solutions. The resulting filtrates were analyzed on a spectrophotometer at the MO maximum absorption wavelength of 464 nm for the remaining MO concentration. As a comparison, the photocatalytic properties of pure Bi_2O_3 and Cu_2O were also evaluated in the same way.

3. Results and discussion

3.1. Synthetic Principle of Cu_2O/Bi_2O_3 composites

As described in the Experimental Section, Cu_2O/Bi_2O_3 composites are synthesized by a ball-milling solid-state chemical reaction method. During the process of ball milling, reactant powder particles repeatedly occurs deformation, fracture and welding in collision events of the ball and powders [16], leading to rapid nucleation followed by slow crystal growth to obtain Cu_2O/Bi_2O_3 composite nanoparticles. The chemical reaction processes for the formation of Cu_2O/Bi_2O_3 composite can be formulated as the following:

$$CuCl + NaOH \xrightarrow{\text{ball-milling}} CuOH + NaCl$$

$$Bi(NO_3)_3 \cdot 5H_2O + xNaOH \xrightarrow{\text{ball-milling}} BiONO_3 \cdots \xrightarrow{\text{ball-milling}} Bi_2O_3 \cdot nH_2O + NaNO_3$$

$$2CuOH + Bi_2O_3 \cdot nH_2O \xrightarrow{\text{ball-milling}} Cu_2O/Bi_2O_3 + (n+1)H_2O$$

3.2. Influence of ball-milling time on formation of Cu_2O/Bi_2O_3 composite

Fig.1 shows the XRD patterns of the products obtained in a 1:3:13 molar ratio of CuCl: $Bi(NO_3)_3{\cdot}5H_2O$: NaOH at the ball-milling times of 0.5, 1, 2, and 4 h, respectively. As you can see from Fig.1, all synthesized products are composed of Cu_2O and Bi_2O_3, which diffraction peaks are indexed to cubic Cu_2O phase (JCPDS No. 78-2076) and monoclinic alpha-Bi_2O_3 phase (JCPDS No. 72-0398), respectively. With the increase of milling time, the diffraction peaks of Cu_2O ((111) peak at 36.44° of 2θ) and Bi_2O_3 ((120) peak at 27.48° of 2θ) increase distinctly, indicating an increase of crystallinity of Cu_2O and Bi_2O_3. In Cu_2O/Bi_2O_3 composite, the mean crystallite sizes of Cu_2O are ca. 11.2, 14.1, 16.3 and 19.1 nm, and those of Bi_2O_3 are ca. 21.4, 26.1, 31.3 and 38.2 nm, corresponding to the ball-milling times of 0.5, 1, 2 and 4 h, respectively, which are calculated from the Seherrer's formula. It shows the increase of the mean crystallite sizes of Cu_2O and Bi_2O_3 with increasing the ball-milling time, indicating the nano-scale Cu_2O/Bi_2O_3 composites with controllable sizes can be produced by controlling the ball milling time.

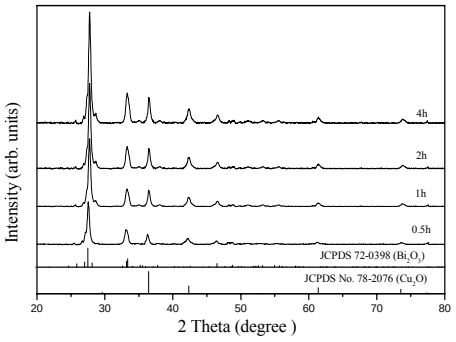

Fig.1. XRD patterns of the products obtained at different ball-milling times.

3.3. Influence of NaOH content on formation of Cu_2O/Bi_2O_3 composite

Fig.2 shows the XRD patterns of the products obtained at 2 h ball-milling time in the different molar ratios of CuCl:$Bi(NO_3)_3{\cdot}5H_2O$:NaOH (1:3:11, 1:3:13, 1:3:15 and 1:3:20). From Fig. 2, it can be seen that the diffraction peaks of Bi_2O_3 and Cu_2O broaden and decrease gradually as the molar ratios of CuCl to NaOH decrease. The mean crystallite sizes of Cu_2O calculated from the Seherrer's formula decrease from 18.7 to 12.2 nm and those of Bi_2O_3 from 33.3 to 27.7 nm, corresponding to the decrease of the molar ratios of CuCl: $Bi(NO_3)_3{\cdot}5H_2O$: NaOH from 1:3:11 to 1:3:20, indicating the decrease in the crystallite size of Bi_2O_3 and Cu_2O at elevated NaOH contents. It can be explained that an increase in NaOH content will speed up the ball-mill reaction between NaOH and CuCl or $Bi(NO_3)_3{\cdot}5H_2O$, causing the nucleation faster rate than growth rate, which is responsible for the decreases of the crystallite size of Bi_2O_3 and Cu_2O.

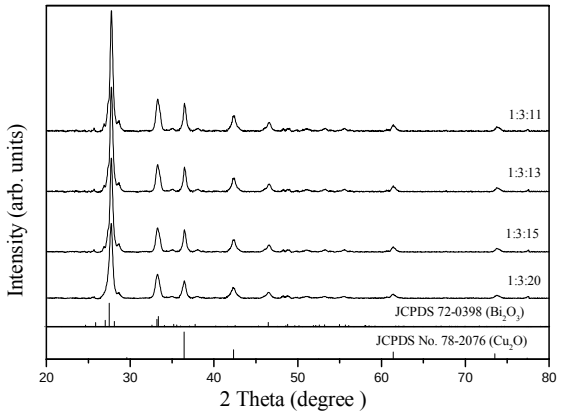

Fig.2. XRD patterns of the products obtained in the different molar ratios of CuCl:$Bi(NO_3)_3{\cdot}5H_2O$:NaOH.

3.4. Optical property of Cu_2O/Bi_2O_3 composite

The optical absorption properties of the photocatalysts play an important role in the photocatalytic activity [7]. The optical absorbance spectrum of the Cu_2O/Bi_2O_3 sample synthesized at 2h ball-milling time in the molar ratio of 1:3:13 for CuCl:$Bi(NO_3)_3{\cdot}5H_2O$:NaOH is obtained using a doubled-beam UV-visible spectrophotometer equipped with an integrating sphere. The UV-Vis diffuse reflectance spectrum (DRS) of Cu_2O/Bi_2O_3 is recorded using $BaSO_4$ as a reference and is converted from reflection to absorbance by Kubelka-Munk method. For comparison purposes, those of pure Bi_2O_3 and pure Cu_2O are also obtained. Fig. 3 demonstrates that the optical absorbance spectra of Bi_2O_3, Cu_2O and Cu_2O/Bi_2O_3 samples.

In Fig. 3, all the samples absorb visible light, suggesting that the light absorption properties of Bi_2O_3, Cu_2O and Cu_2O/Bi_2O_3 are rather similar. What is more, the optical absorption band edge of the Cu_2O/Bi_2O_3 composite exhibits a red shift with respect to those of pure Bi_2O_3 and pure Cu_2O, which might lead to enhanced visible light photocatalytic activity of the Cu_2O/Bi_2O_3 composite.

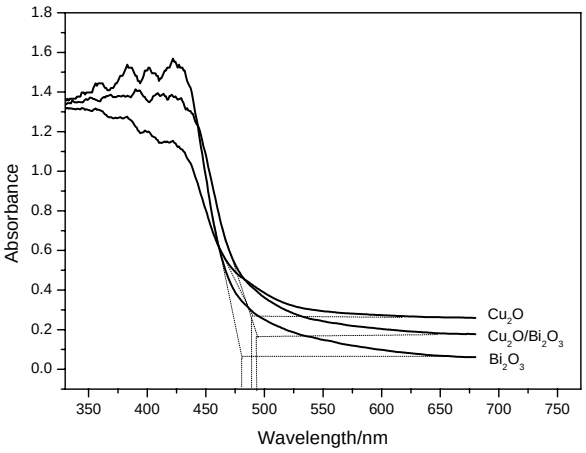

Fig.3. Optical absorption properties of the photocatalysts.

3.5. Photocatalytic property of Cu_2O/Bi_2O_3 composite

The photocatalytic activity of the Cu_2O/Bi_2O_3 composite is evaluated by the photodegradation of MO under visible light irradiation and is compared with that of pure Bi_2O_3 and Cu_2O. Fig. 4 illustrates the activity comparison of the Cu_2O/Bi_2O_3 composite, pure Bi_2O_3 and Cu_2O. It can be seen that the degradation rate of MO over the catalysts can be arranged in the order of Cu_2O/Bi_2O_3 > Cu_2O > Bi_2O_3. The higher activity of the Cu_2O/Bi_2O_3 composite as compared with each component is ascribed to the following two reasons. Firstly, the introduction of Cu_2O into Bi_2O_3 results in better harvest of visible light, which is verified by the UV-Vis diffuse reflectance spectra, and as a results the Cu_2O/Bi_2O_3 composite generates more electrons and holes than each component under visible light irradiation, leading to the formation of more reactive radicals such as superoxide radicals ($\cdot O_2^-$) and hydroxide radicals (·OH) to facilitate the decomposition of MO. Secondly, the more efficient separation of photogenerated electrons and holes in the Cu_2O/Bi_2O_3 composite can be responsible for the high photocatalytic activity of the Cu_2O/Bi_2O_3 composite. The detail photodegradation mechanism is demonstrated in Section 3.6.

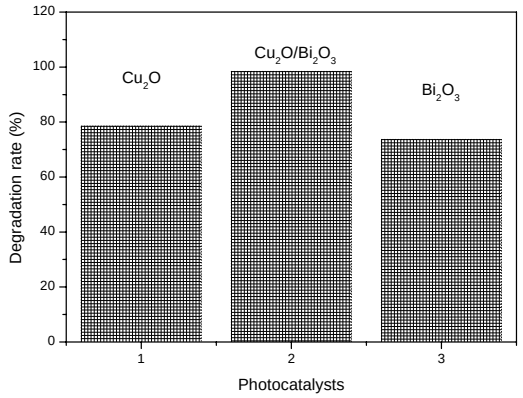

Fig.4. Photocatalytic degradation of MO over the Cu_2O/Bi_2O_3, Bi_2O_3 and Cu_2O.

3.6. Possible mechanism for enhanced photocatalytic performance of Cu_2O/Bi_2O_3 composite

In order to investigate the mechanism of the enhanced photocatalytic activity of the Cu_2O/Bi_2O_3 composite, it is necessary to confirm the relative band positions of the two semiconductors, because the band edge potential positions play an important role in determining the migration direction of the photogenerated charge carriers [17]. The band edge potential positions of conduction band (CB) and valance band (VB) of Cu_2O are -0.28 and +1.92 eV [15], and of Bi_2O_3 are +0.33 and +3.13 eV [18] respectively, which are schematically illustrated in Fig. 5.

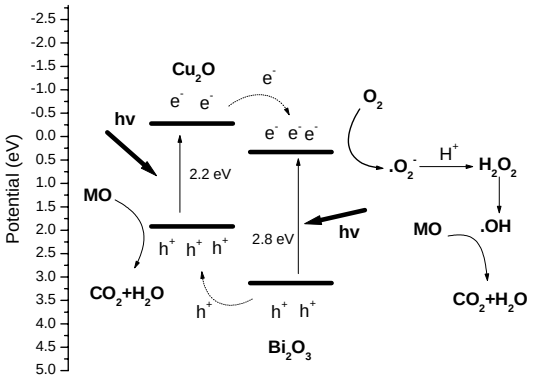

Fig.5. Band gap structures of Cu_2O and Bi_2O_3, and the possible process for the separation of charge carriers.

According to the schema of Fig. 5, when the system is irradiated under visible light, Cu_2O and Bi_2O_3 are excited simultaneously and the electrons (e^-) in the VB are excited to the CB, with the same amount of holes (h^+) left in VB in both Cu_2O and Bi_2O_3. Meanwhile, the excited electrons can easily transfer from the CB of Cu_2O to the CB of Bi_2O_3, because the CB edge potential position of Cu_2O (-0.28 eV) is more negative than that of Bi_2O_3 (+0.33 eV). On the other hand, because the VB edge potential position of Bi_2O_3 (+3.13 eV) is more positive than that of Cu_2O (+1.92 eV), the holes on the VB edge of Bi_2O_3 will transfer to that of Cu_2O. In such way, it is expect to achieve an efficient separation of the photoinduced electrons and holes, greatly reducing the recombination of the photogenerated charge carriers. Consequently, the enhanced photocatalytic activity of the Cu_2O/Bi_2O_3 composite can be achieved. Generally, the more the photoinduced electrons and holes, the more reactive radicals such as hydroxide radicals (·OH) and superoxide radicals ($\cdot O_2^-$) are formed [15]. It has been reported that ·OH, $\cdot O_2^-$ and h^+ are powerful oxidative species and oxidize dyes to intermediates and finally to CO_2 and H_2O [19-22]. In the photocatalytic degradation of MO over the Cu_2O/Bi_2O_3 composite, Cu_2O/Bi_2O_3 is first excited under visible light and produce charge carriers. Then, the accumulated photoinduced electrons in the CB of Bi_2O_3 can be captured by O_2 adsorbed on the surface to yield $\cdot O_2^-$, which might combine with H^+ to form H_2O_2, and subsequently form ·OH [23, 24]. Finally, both ·OH and the accumulated photoinduced holes in Cu_2O will completely oxidize MO into to CO_2 and H_2O. The photocatalytic processes are described in the following expressions:

$$Cu_2O / Bi_2O_3 \xrightarrow{hv} h^+ + e^-$$
$$O_2 + e^- \longrightarrow \cdot O_2^-$$
$$\cdot O_2^- + e^- + 2H^+ \longrightarrow H_2O_2$$
$$H_2O_2 + e^- \longrightarrow \cdot H + OH^-$$
$$h^+ + OH^- \longrightarrow \cdot OH$$
$$MO + h^+(\cdot OH) \longrightarrow \text{intermediates} \rightarrow CO_2 + H_2O$$

4. Conclusions

In this work, a visible-light-driven Cu_2O/Bi_2O_3 nanocomposite has been successfully synthesized at room temperature by a facile one-step solid-state reaction method. Both ball-milling time and NaOH content play key roles in the formation of nanostructure Cu_2O/Bi_2O_3 with controllable sizes. The as-synthesized Cu_2O/Bi_2O_3 composite shows higher photocatalytic activity than its single component in the degradation of MO under visible light irradiation. The enhanced photocatalytic activity of Cu_2O/Bi_2O_3 composite is generally attributed to the effective separation of photoinduced electron-hole pairs, leading to more reactive species produced by the composite than by its components. This study not only provides a new route to synthesize Cu_2O/Bi_2O_3 nanocomposite photocatalysts, but also provides high efficient visible-light-driven photocatalysts for water purification and environmental remediation.

Acknowledgments

This work is financially supported by Anhui

Provincial Natural Science Foundation (No. 1208085MB30), Natural Science Foundation of Anhui Provincial Department of Education (Nos. KJ2013A231, KJ2014A230, and KJ2010A302), and open fund (OGL-201213) of State Key Laboratory of Organic Geochemistry, Guangzhou Institute of Geochemistry, Chinese Academy of Sciences, Guangzhou, China.

References

[1] X. B. Chen, C. Li, M. Grätzel, R. Kostecki, S. S. Mao, Chem Soc Rev **41**, 7909(2012).
[2] H. Tong, S. X. Ouyang, Y. P. Bi, N. Umezawa, M. Oshikiri, J. H. Ye, Adv Mater **24**, 229(2012).
[3] T. Saison, N. Chemin, C. Chanéac, O. Durupthy, V. Ruaux, L. Mariey, F. Maugé, P. Beaunier, J. P. Jolivet, J Phys Chem C **115**, 5657(2011).
[4] A. M. Abdulkarem, A. A. Aref, A. Abdulhabeeb, Y. F. Li, Y. Yu, J Alloys Compd **560**, 132 (2013).
[5] W. F. Yao, H. Wang, X. H. Xu, X. F. Cheng, J. Huang, S. X. Shang, X. N. Yang, M. Wang, Appl Catal A **243**, 185(2003).
[6] M. Long, W. Cai, J. Cai, B. Zhou, X. Chai, Y. Wu, J Phys Chem B **110**, 20211(2006).
[7] J. L. Hu, H. M. Li, C. J. Huang, M. Liu, X. Q. Qiu, Appl Catal B **142-143**, 598(2013).
[8] L. Chen, Q. Zhang, R. Huang, S. F. Yin, S. L. Luo, C. T. Au, Dalton Trans **41**, 9513(2012).
[9] M. Ge, Y. Li, L. Liu, Z. Zhou, W. Chen, J Phys Chem C **115**, 5220(2011).
[10] A. Hameed, V. Gombac, T. Montini, M. Graziani, P. Formasiero, Chem Phys Lett **472**, 212(2009).
[11] S. Y. Chai, Y. J. Kim, M. H. Jung, A. K. Chakraborty, D. Jung, W. Lee, J Catal **262**, 144(2009).
[12] Y. Li, J. Wang, H. Yao, L. Dang, Z. Li, Catal Commun **12**, 660(2011).
[13] L. Zhu, B. Wei, L. Xu, Z. LÜ, H. Zhang, H. Gao, J. Che, Cryst Eng Commun **14**, 5705(2012).
[14] J. Z. Li, J. B. Zhong, X. Y. He, S. T. Huang, J. Zeng, J. J. He, W. L. Shi, Appl Surf Sci **284**, 527(2013).
[15] Q. Yuan, L. Chen, M. Xiong, J. He, S. L. Luo, C. T. Au, S. F. Yin, Chem Eng J **255**, 394(2014).
[16] P. G. McCormick, T. Tsuzuki, J. S. Robinson, J. Ding, Adv Mater **12**, 1008(2001).
[17] L. Chen, S. F. Yin, S. L. Luo, R. Huang, Q. Zhang, T. Hong, P. C. T. Au, Ind Eng Chem Res **51**, 6760(2012).
[18] A. M. Abdulkarem, J. Li, A. A. Aref, L. Ren, E. M. Elssfah, H. Wang, Y. Ge, Y. Yu, Mater Res Bull **46**, 1443(2011).
[19] Y. N. Wang, K. J. Deng, L. Z. Zhang, J Phys Chem C **115**, 14300(2011).
[20] Y. Hu, D. Z. Li, Y. Zheng, W. Chen, Y. H. He, Y. Shao, X. Z. Fu, G. C. Xiao, Appl Catal B **104**, 30(2011).
[21] C. S. Guo, M. Ge, L. Liu, G. D. Gao, Y. C. Feng, Y. Q. Wang, Environ Sci Technol **44**, 419(2010).
[22] C. Y. Wang, H. Zhang, F. Li, L. Y. Zhu, Environ Sci Technol **44**, 6843(2010).
[23] N. Wetchakun, S. Chaiwichain, B. Inceesungvorn, K. Pingmuang, S. Phanichphant, A. I. Minett, J. Chen, Acs Appl Mater Inter **4**, 3718(2012).
[24] P. Ju, P. Wang, B. Li, H. Fan, S. Y. Ai, D. Zhang, Y. Wang, Chem Eng J **236**, 430(2014).

*Corresponding author: mlzhang1268@163.com